Solvent-Selective Reactions of Alkyl Iodide with Sodium Azide for Radical Generation and Azide Substitution and Their Application to One-Pot Synthesis of Chain-End Functionalized Polymers

Chen-Gang Wang, Atsushi Goto*

Division of Chemistry and Biological Chemistry, School of Physical and Mathematical Sciences, Nanyang Technological University, 21 Nanyang Link, 637371 Singapore

ABSTRACT: Herein, a new reaction of an alkyl iodide (R–I) with an azide anion (N_3^-) to reversibly generate the corresponding alkyl radical ($R^\bullet$) is reported. Via this new reaction, N_3^- was used as an efficient catalyst in living radical polymerization, yielding a well-defined polymer-iodide. A particularly interesting finding was the solvent selectivity of this reaction; namely, R–I and N_3^- generated $R^\bullet$ in non-polar solvents, while the substitution product R–N_3 was generated in polar solvents. Exploiting this unique solvent selectivity, a one-pot synthesis of polymer–N_3 was attained. N_3^- was first used as a catalyst for living radical polymerization in a non-polar solvent to produce a polymer-iodide and was subsequently used as a substitution agent in a polar solvent by simply adding the polar solvent, thereby transforming the polymer-iodide to polymer–N_3 in one pot. This one-pot synthesis was further applied to obtain N_3-chain-end-functionalized polymer brushes on surface, uniquely controlling the N_3 coverage (number density). Using the chain-end N_3, the obtained linear and brush polymers were connected to functional molecules via an azide-alkyne click reaction. The attractive features of this system include facile operation, access to unique polymer designs, and no requirement for using excess NaN_3. In addition to N_3^-, thiocyanate ($^-$SCN) and cyanate ($^-$OCN) anions were also studied.

INTRODUCTION

Solvent-selective reactions offer unique synthetic approaches in organic chemistry.[1–4] In different solvents, different products are selectively generated from the same reactant. Solvent is one of the most useful stimuli that can switch the reactions from one to another. Thus, multiple reactions may be regulated in one pot by simply altering the solvent qualities.

A reaction of an alkyl halide (R–X) with sodium azide (NaN_3) is useful for synthesizing an alkyl azide (R–N_3).[5] The subsequent copper-catalyzed cycloaddition of R–N_3 and an alkyne is a so-called "click" reaction and is extensively exploited to connect various molecules to R.[6,7]

Scheme 1. One-pot synthesis of N_3-chain-end functionalized polymer via solvent-dependent dual works of NaN_3.

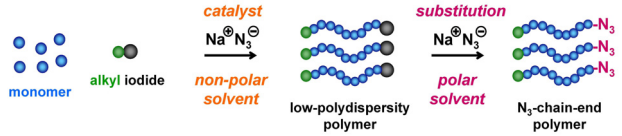

Our research group is interested in the generation of a carbon-centered radical ($R^\bullet$) from an alkyl iodide (R–I) using a catalyst.[8–12] In this paper, we report the unprecedented finding that the reaction of R–I with NaN_3 generated not only R–N_3 but also $R^\bullet$ with a catalytic role of NaN_3. A particularly interesting finding was the solvent selectivity of this reaction. Namely, $R^\bullet$ was generated in non-polar solvents, and R-N_3 was generated in polar solvents selectively. This finding inspired us with a unique application, i.e., the one-pot synthesis of azide-chain-end-functionalized polymers by selectively controlling the two reactions with solvents (Scheme 1), as described below.

Chain-end-functionalized polymers are employed in many applications.[13,14] Because chain-end-functionalized polymers can be connected with other polymers, they are used as building blocks for synthesizing novel block copolymers as well as star, comb, and network polymers. They can also be connected to small molecules and biomolecules and also onto solid surfaces to generate polymer brushes on the surfaces. Chain-end-functionalized polymers can thus create novel materials.

Scheme 2. Reversible activation: (a) General scheme, (b) catalysis with I^-, and (c) catalysis with N_3^-.

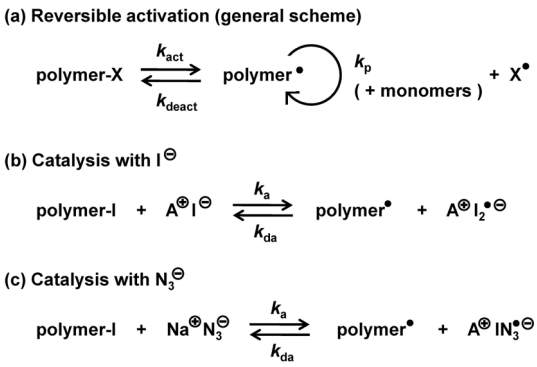

Living radical polymerization (LRP) is a useful method for synthesizing low-polydispersity polymers with well-defined structures.[15–30] LRP is based on the reversible activation of a dormant species (polymer−X) to a propagating radical (polymer$^\bullet$) (Scheme 2a). A range of chain-end functionalized poly-

mers are synthesized by the post-transformation of the capping agent X to functional groups.

Atom transfer radical polymerization (ATRP) utilizes chloride and bromide as X and yields polymer-chloride and polymer-bromide chains.[17–20] The post-transformation of these polymer chains with NaN_3 efficiently provides polymer-azide (polymer−N_3), and applications of polymer−N_3 have been extensively developed.[31,32] Polystyrene and polyacrylates are used in most cases. Polymethacrylates are rarely used, likely because of the low reactivity of the nucleophilic substitution of N_3 for the tertiary alkyl chloride and bromide. A literature used a 10-fold excess of NaN_3 to convert polymethacrylate-bromide to polymethacrylate-N_3.[33] The use of a large amount of azide causes potential safety problems and limits the synthesis of polymethacrylate-N_3. Polymethacrylate-N_3 is highly desirable but its synthesis is still challenging.

We previously reported that R–I reversibly generates $R^\bullet$ in the presence of iodide anion (I^-) (as a catalyst).[8,9] Several organic and alkali-metal salts such as tetrabutylammonium iodide ($Bu_4N^+I^-$ (BNI))[8] and sodium iodide (NaI)[9] were employed as catalysts. Such a role of I^- had been unprecedented in chemistry. We utilized this reaction to the reversible activation of polymer−I to polymer$^\bullet$ and developed a new LRP system (Scheme 2b), where X is iodide and the catalyst is I^-. This LRP system is attractive because no special capping agents or expensive catalysts are required.

Based on our previous study, we wondered whether pseudo-halides such as an azide anion (N_3^-) could also work as catalysts for the reversible generation of $R^\bullet$ from R–I (Scheme 2c). The use of N_3^- in such a manner is new in chemistry. We suppose that N_3^- coordinates the iodide of R–I to form an R–I/N_3^- complex and that R–I/N_3^- subsequently releases $R^\bullet$ and $I^\bullet/N_3^-$. This is the first use of halogen bonding (non-covalent bonding of halogen and nitrogen) between R–I and N_3^- to generate $R^\bullet$. The concept of halogen bonding has gained increased recognition, particularly in crystal engineering.[34,35]

While our system is reversible, the irreversible generation of $R^\bullet$ from alkyl halides using organic[36–38] and $SO_2^{-\bullet}$[39] radical anions through single electron transfer (SET) was reported. The $SO_2^{-\bullet}$ system was used to initiate SET-degenerative chain transfer (SET-DT) polymerization.[39]

In this paper, we report the unique reaction of R–I with N_3^- to reversibly generate $R^\bullet$ and the application of N_3^- as a useful catalyst in LRP. We found that not only N_3^- but also thiocyanate ($^-$SCN) and cyanate ($^-$OCN) anions work as catalysts. The catalysts are amenable to a range of monomers encompassing methacrylates, acrylates, and functional monomers. A particularly significant finding was the solvent selectivity of this reaction; namely, R–I and the pseudo-halides can generate $R^\bullet$ in non-polar solvents and substitution products (R−N_3 and R−SCN) in polar solvents. The radical generation and substitution reactions can be switched by simply altering the solvent polarity. A unique application of this solvent selective reaction presented in this paper is the one-pot synthesis of N_3-chain-end-functionalized polymers with the dual use of N_3^- for conducting the LRP in "non-polar" solvents (catalyst) and the subsequent chain-end transformation in "polar" solvents (substitution agent) by simply adding polar solvents after the LRP. The one-pot synthesis was further applied to obtain N_3-chain-end-functionalized polymer brushes on a surface, enabling unique control of the N_3 coverage (number density). Notably, this approach also enabled us to synthesize N_3-chain-end polymethacrylates without using a large excess of azide, overcoming the challenge mentioned above.

RESULTS AND DISCUSSION

Experimental Proof of the Generation of $R^\bullet$ from R−I Using NaN_3. A radical trap experiment[8,40–42] was performed to confirm the generation of $R^\bullet$ from R−I catalyzed by NaN_3. 2-Iodo-2-methylpropionitrile (CP−I) (Figure 1) was used as an R−I. We heated CP−I (20 mM), NaN_3 (20 mM), 18-*crown*-6-ether (20 mM), and 2,2,6,6-tetramethylpiperidine-1-oxyl (TEMPO) (40 mM) as a radical trap in toluene-d_8 at 70 °C. 18-*crown*-6-Ether was used to dissolve NaN_3 in the non-polar solvent (toluene-d_8). If CP–I reacts with NaN_3, the generated radical CP$^\bullet$ is trapped by TEMPO, thereby yielding CP–TEMPO. Figure 2a shows the ^{1}H NMR spectrum of the reaction mixture. After 3 h, new signals appeared and matched those of pure CP−TEMPO that was independently prepared. No substitution product, CP−N_3, was generated. (Figures 2c and 2d show the spectrum of pure CP−I and CP−N_3, respectively, for reference.) The result clearly demonstrates the generation of $R^\bullet$ from R–I using NaN_3 in a selective manner in the non-polar solvent.

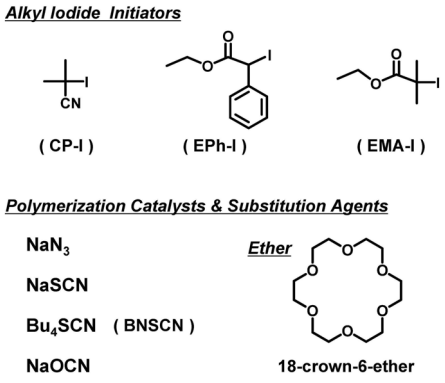

Figure 1. Structures of alkyl iodides, catalysts & substitution agents, and crown ether used in this work.

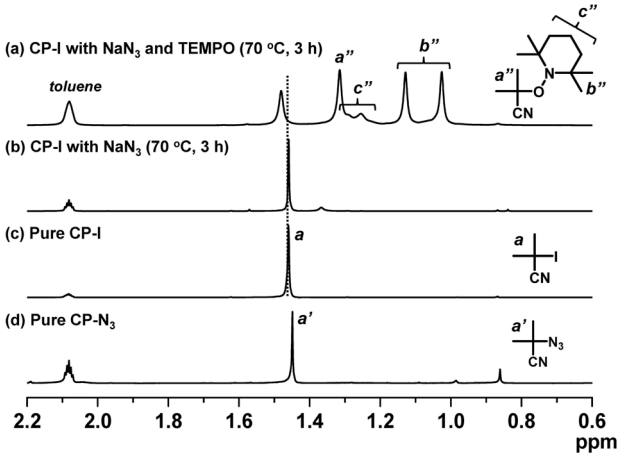

Figure 2. ^{1}H NMR (500 MHz) spectra of toluene-d_8 solutions. (a) CP-I (20 mM), NaN_3 (20 mM), crown-ether (20 mM), and TEMPO (40 mM) heated at 70 °C for 3 h, (b) CP-I (20 mM), NaN_3 (20 mM), and crown-ether (20 mM) heated at 70 °C for 3 h, (c) pure CP-I, and (d) pure CP-N_3.

Figure 2b shows the same reaction but without TEMPO. Virtually 100% of the CP−I remained. This result means that the generation of CP$^{\bullet}$ from CP−I with NaN_3 is reversible. Again, no CP−N_3 was generated. Taking advantage of this reversible nature, we utilized NaN_3 as a catalyst for the polymerization (LRP), as described later.

Solvent-Selective Reaction of R−I with NaN_3. We found that the reaction of R−I with NaN_3 selectively yields R−N_3 in polar solvents and R$^{\bullet}$ in non-polar solvents. We used ethyl 2-iodo-2-methylpropionate (EMA−I (Figure 1)) as an R−I, which is a unimer model of polymethacrylate-iodide. We heated EMA−I (20 mM), NaN_3 (20 mM), and 18-*crown*-6-ether (20 mM). Dimethyl sulfoxide (DMSO)-d_6 was used as a polar solvent, while a mixture of toluene-d_8 (70%) and acetone-d_6 (30%) was used as a non-polar solvent. This mixture of toluene-d_8 (dielectric constant ε = 2.4) and acetone-d_6 (ε = 20.7) is a model of methyl methacrylate (MMA) medium (ε = 7.9).

Figure 3a shows the reaction in DMSO-d_6 heated at 50 °C for 1 h. EMA−I was quantitatively (100%) converted to EMA−N_3 (Figure 3c), and no EMA−I (Figure 3b) remained. Figure 3d shows the reaction in the toluene-d_8/acetone-d_6 mixture at 50 °C for 1 h. Only 11% of EMA−I was converted to EMA−N_3 (Figure 3f), and most (89%) of EMA−I (Figure 3e) remained. The remaining EMA−I underwent only a reversible generation of EMA$^{\bullet}$. (Virtually no radical-radical termination product of EMA$^{\bullet}$ was observed, because of the low concentration of EMA$^{\bullet}$.) These results demonstrate that the reaction of R–I with NaN_3 can be selectively controlled to generate EMA−N_3 in polar solvents and R$^{\bullet}$ in non-polar solvents.

Polymerizations of MMA Using NaN_3 as a Catalyst. We exploited the catalytic role of NaN_3 (to reversibly generate R$^{\bullet}$ from R−I) in the LRP of MMA. MMA is a non-polar medium. We heated a mixture of MMA (8 M), CP–I (80 mM) as a low-mass dormant species (alkyl iodide initiator), NaN_3 (40 mM) as a catalyst, and 18-*crown*-6-ether (40 mM) for the dissolution of NaN_3 at 70 °C.

Although the exact mechanism for the reversible activation with NaN_3 remains unclear, we suppose the following scheme. $Na^+N_3^-$ activates polymer−I, thereby generating polymer$^{\bullet}$ and $Na^+(IN_3^{\bullet-})$ (Scheme 3a). A few monomers are added to polymer$^{\bullet}$ until polymer$^{\bullet}$ is deactivated to regenerate polymer−I. Because $Na^+(IN_3^{\bullet-})$ is not a stable radical, two $Na^+(IN_3^{\bullet-})$ species may react with each other to produce $Na^+N_3^-$ and $Na^+(I_2N_3^-)$ as stable species (Scheme 3b). $Na^+N_3^-$ acts as an activator, whereas $Na^+(I_2N_3^-)$ acts as a deactivator (Scheme 3c). Polymer$^{\bullet}$ can thus be deactivated by either $Na^+(IN_3^{\bullet-})$ (Scheme 3a) or $Na^+(I_2N_3^-)$ (Scheme 3c). The activation-deactivation cycles are repeated, and hence the polymer chain grows little by little, yielding a low-polydispersity polymer. Again, this supposed mechanism is not definitive, and the exact mechanism needs be clarified.

Scheme 3. Possible mechanism of reversible activation with N_3^- catalyst.

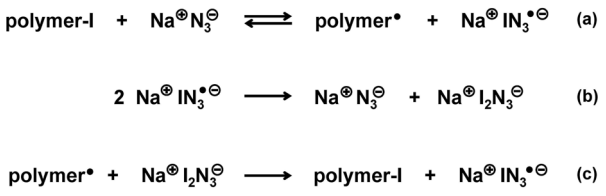

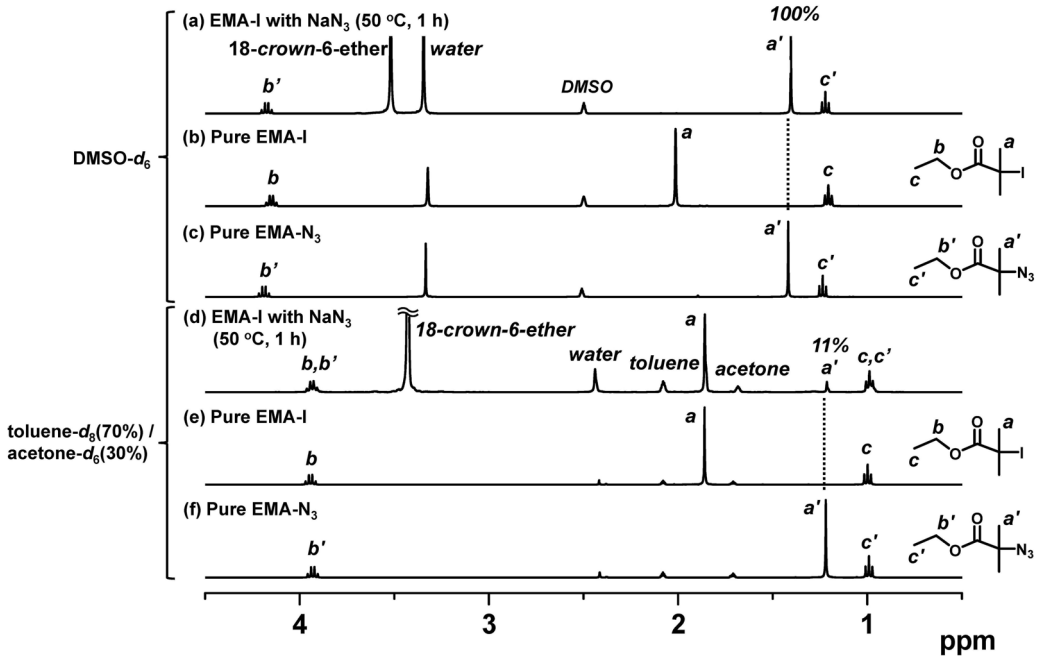

Figure 3. ^{1}H NMR (500 MHz) spectra in (a-c) DMSO-d_6 and (d-f) a mixture of toluene-d_8 (70%) and acetone-d_6 (30%). (a and d) EMA-I (20 mM), NaN_3 (20 mM), and crown-ether (20 mM) heated at 50 °C for 1 h, (b and e) pure EMA-I, and (c and f) pure EMA-N_3.

Table 1. Bulk Polymerizations of MMA with R–I, Catalyst, and Crown Ether.

Entry	Target DP[a]	R−I	Catalyst	$[MMA]_0/[CP-I]_0/[catalyst]_0/[crown\ ether]_0/[I_2]_0$ (mM)	T (°C)	t (h)	Conv (%)	M_n ($M_{n,theo}$[b])	PDI
1	100	CP−I	NaN_3	8000/80/40/40/0	70	5	80	7900 (8000)	1.26
2	100	CP−I	NaN_3	8000/80/40/40/1	70	6	91	9400 (9100)	1.24
3	100	CP−I	NaSCN	8000/80/40/40/1	70	10	78	8000 (7800)	1.15
4	100	CP−I	BNSCN	8000/80/40/0/1	70	10	75	7300 (7500)	1.24
5	100	CP−I	NaOCN	8000/80/160/160/1	70	8	75	8000 (7500)	1.28
6	200	CP−I	NaN_3	8000/40/40/40/1	70	10	84	20000 (17000)	1.33
7	400	CP−I	NaN_3	8000/20/40/40/1	70	24	88	42000 (36000)	1.42
8	100	EPh−I	NaN_3	8000/80/40/40/0	70	5	92	10300 (9200)	1.30
9	100	EMA−I	NaN_3	8000/80/40/40/0	70	8	79	17000 (7900)	1.70
10	100	EMA−I	NaN_3	8000/80/40/40/3	70	24	91	9100 (9600)	1.39
C1	100	CP−I	BNI	8000/80/40/0/0	70	4	91	9400 (9100)	1.21

[a] Target degree of polymerization at 100% monomer conversion (calculated by $[MMA]_0/[CP-I]_0$). [b] Theoretical M_n calculated with $[MMA]_0$, $[CP-I]_0$, and monomer conversion.

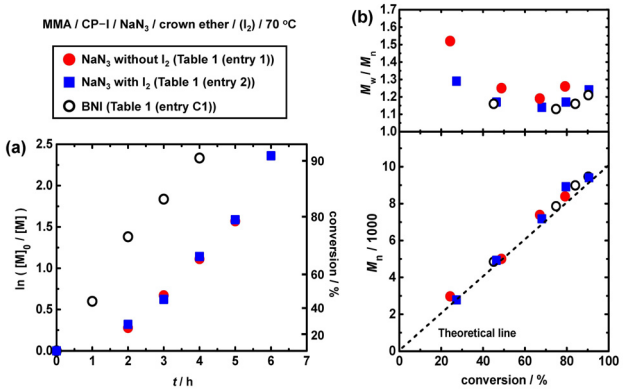

Figure 4. Plots of (a) $\ln([M]_0/[M])$ vs t and (b) M_n and M_w/M_n vs conversion for the MMA/CP-I/NaN_3/crown ether/(I_2) and MMA/CP-I/BNI systems (70 °C): $[MMA]_0$ = 8 M; $[CP\text{-}I]_0$ = 80 mM; $[NaN_3]_0$ = 40 mM; $[crown\ ether]_0$ = 40 mM; $[I_2]_0$ = 0 or 1 mM, or $[MMA]_0$ = 8 M; $[CP\text{-}I]_0$ = 80 mM; $[BNI]_0$ = 40 mM. The symbols are indicated in the figure.

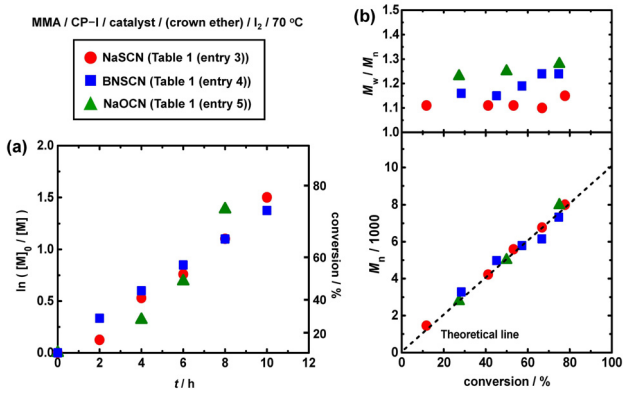

Figure 5. Plots of (a) $\ln([M]_0/[M])$ vs t and (b) M_n and M_w/M_n vs conversion for the MMA/CP-I/catalyst/(crown ether)/I_2 systems (70 °C): $[MMA]_0$ = 8 M; $[CP\text{-}I]_0$ = 80 mM; $[catalyst]_0$ = 40 or 160 mM; $[crown\ ether]_0$ = 0, 40, 160 mM; $[I_2]_0$ = 1 mM. The symbols are indicated in the figure.

Figure 4 (filled circles) and Table 1 (entry 1) show the polymerization result. The polymerization proceeded up to 80% monomer conversion in 5 h, confirming the generation of the carbon-centered radical (the propagating radical) from CP–I and NaN_3. No polymerization proceeded without CP–I or NaN_3, again confirming that the radical was generated by the combination of CP–I and NaN_3. However, the polydispersity index (PDI) (= M_w/M_n) was larger than 1.5 at an early stage of polymerization (Figure 4 (filled circles)), where M_w and M_n were the weight- and number-average molecular weights, respectively. This is because a sufficient amount of the deactivator $Na^+(I_2N_3^-)$ did not accumulate at an early stage of polymerization, at which many monomers added to polymer$^\bullet$.

Therefore, we added a small amount of molecular iodine (I_2), which forms $Na^+(I_2N_3^-)$ with NaN_3. In fact (Figure 4 (squares) and Table 1 (entry 2)), with the addition of 1 mM of I_2 (as little as 1/40 equivalent to NaN_3), M_n agreed with the theoretical value ($M_{n,theo}$) and PDI was approximately 1.3 from an early stage of polymerization. In this case, the degree of polymerization (DP) expected at full (100%) monomer conversion was 100, because the $[MMA]_0/[CP-I]_0$ ratio was set to 100. Importantly, PDI also remained small (approximately 1.2) up to high conversions (nearly 90%), thereby illustrating the success of this LRP. Figure 4 (open circles) and Table 1 (entry C1) show the same polymerization but using BNI ($Bu_4N^+I^-$)[9] which is one of the most effective catalysts previously used in the LRP. NaN_3 led to a slower polymerization than BNI but provided control of the molecular weight and PDI as efficiently as BNI, demonstrating the usefulness of the NaN_3 catalyst. We were able to reduce the amount of NaN_3 from 40 mM (Table 1 (entry 2)) to 5 mM (Supporting Information (Table S1 and Figure S6)) to control PDI, although the polymerization rate decreased with a reduced amount of NaN_3 as expected from the equilibrium in Scheme 2c.

Polymerizations of MMA Using Different Catalysts. Instead of N_3^-, we used $^-$SCN and $^-$OCN as catalysts. Figure 5 and Table 1 (entries 3−5) show the results with NaSCN, $Bu_4N^+(^-SCN)$ (BNSCN) and NaOCN. In all cases, the polymerization proceeded smoothly, M_n well agreed with $M_{n,theo}$, and PDI was small, i.e., approximately 1.2. The cationic counterpart of BNSCN is organic, and hence the polymerization system is completely metal-free. Crown-ether is also unnecessary for BNSCN. Thus, N_3^-, $^-$SCN, and $^-$OCN are all efficient catalysts of LRP.

Toward Higher Molecular Weights. We targeted higher DPs of 200 and 400 (expected at 100% monomer conversion) using NaN_3 (Table 1 (entries 6 and 7) and Supporting Information (Figures S7 and S8)). We obtained low-polydispersity

(PDI = 1.1-1.4) polymers in reasonable periods of time (monomer conversion = 84-88% in 10-24 h). For targeting a DP above 400, it took a longer polymerization time during which the substitution of polymer–I with N_3 became significant, leading to a large PDI.

Other Alkyl Iodide Initiators. Besides CP–I, we used ethyl α-iodophenylacetate (EPh−I) and EMA−I as alkyl iodide initiators (Figure 1) with NaN_3 as a catalyst for the MMA polymerization (Figure 6 and Table 1 (entries 8−10)). A mixture of MMA (8 M), an alkyl iodide (80 mM), NaN_3 (40 mM) and 18-*crown*-6-ether (40 mM) was heated at 70 °C. EPh−I was a highly efficient alkyl iodide initiator (Figure 6 (circles) and Table 1 (entry 8)). The M_n agreed with the theoretical value ($M_{n,theo}$), and the PDI was small (1.1−1.2) from an early stage of polymerization, suggesting the fast initiation from EPh−I. EMA−I exhibited a deviation of M_n from $M_{n,theo}$ and large PDI values (approximately 1.7) (Figure 6 (squares) and Table 1 (entry 9)). In this system, the addition of a small amount (3 mM) of I_2 led to good control of M_n and PDI (= 1.2-1.4) (Figure 6 (triangles) and Table 1 (entry 10)). Thus, EPh−I and EMA−I can also be used with the NaN_3 catalyst.

Acrylate and Other Methacrylates. The monomer scope of the NaN_3 catalyst encompassed other hydrophobic methacrylates with butyl (BMA), lauryl (LMA), and benzyl (BzMA) groups as well as MMA (Table 2 (entries 1-3)). A methacrylate with an amphiphilic poly(ethylene glycol) (PEGMA) group (Table 2 (entry 4)) was also successfully used in a hydrophobic solvent (50% of toluene).

Besides methacrylates, the NaN_3, BNSCN, and NaOCN catalysts were amenable to an acrylate, butyl acrylate (BA), attaining low polydispersity (PDI = 1.2-1.3) (Figure 7 and Table 2 (entries 5-7)). Because the carbon−iodine bond in an acrylate polymer (with a secondary alkyl chain end) is stronger than that in a methacrylate polymer (with a tertiary alkyl chain end), highly reactive catalysts are necessary for controlling the polymerization of acrylate. The successful use of these catalysts to BA demonstrates their high reactivity. The relatively slow polymerization of BA is attributed to the addition of I_2 for controlling the polydispersity.

One-Pot Synthesis of N_3-Chain-End Functionalized Polymers. We carried out a one-pot synthesis of poly(methyl methacrylate)-azide (PMMA−N_3) via the polymerization of MMA in a non-polar solvent (toluene) followed by the addition of a polar solvent (DMF) for the chain-end transformation. We heated a mixture of MMA (8 M), CP–I (270 mM), NaN_3 (300 mM), 18-*crown*-6-ether (300 mM), I_2 (3 mM), and toluene (toluene/MMA = 25/75%) at 70 °C for 3 h (Table 3 (entry 1)). To clearly characterize the chain end, we targeted a relatively short chain and obtained a PMMA−I with M_n = 3100 and PDI = 1.17 at 79% monomer conversion. Without purifying the polymer, we directly added the polar solvent DMF (DMF/polymerization solution = 2/1) to the polymerization solution for the chain-end transformation. PMMA−N_3 was obtained after 12 h at room temperature without significant change of M_n (= 3400) and PDI (= 1.16) through the transformation.

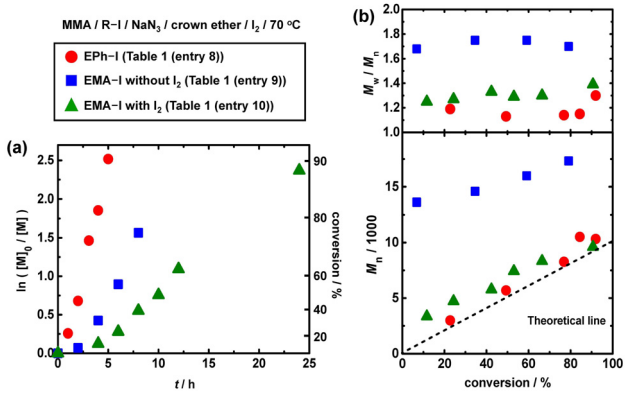

Figure 6. Plots of (a) ln([M]$_0$/[M]) vs t and (b) M_n and M_w/M_n vs conversion for the MMA/R-I/NaN_3/crown ether/I_2 systems (70 °C): [MMA]$_0$ = 8 M; [R-I]$_0$ = 80 mM; [NaN_3]$_0$ = 40 mM; [crown ether]$_0$ = 40 mM; [I_2]$_0$ = 0 or 3 mM. The symbols are indicated in the figure.

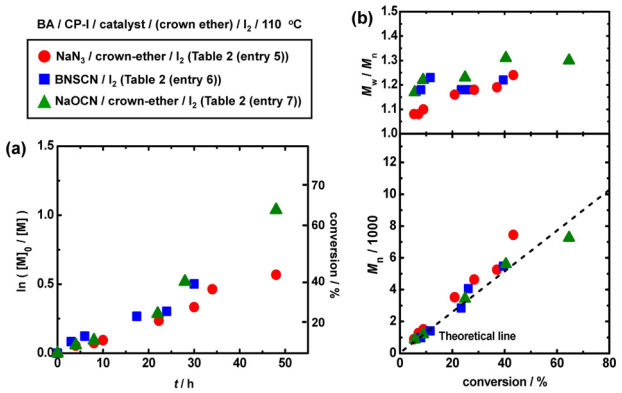

Figure 7. Plots of (a) ln([M]$_0$/[M]) vs t and (b) M_n and M_w/M_n vs conversion for the BA/CP-I/catalyst/(crown ether)/I_2 systems (110 °C): [BA]$_0$ = 8 M; [CP-I]$_0$ = 80 mM; [catalyst]$_0$ = 20, 40, or 80 mM; [crown ether]$_0$ = 0, 40, or 80 mM; [I_2]$_0$ = 2 or 10 mM. The symbols are indicated in the figure.

Table 2. Bulk Polymerizations of Several Monomers with CP−I, Catalyst, and Crown Ether.

Entry	Monomer	Target DP[a]	Catalyst	[M]$_0$/[CP−I]$_0$/[catalyst]$_0$/ [crown ether]$_0$/[I_2]$_0$ (mM)[b]	T (°C)	t (h)	Conv (%)	M_n[c] ($M_{n,theo}$[d])	PDI[c]
1	BMA	100	NaN_3	8000/80/40/40/0	70	24	78	12000 (11000)	1.32
2	LMA	100	NaN_3	8000/80/40/40/0	70	90	51	17000 (13000)	1.29
3	BzMA	100	NaN_3	8000/80/40/40/0	70	12	72	13000 (13000)	1.33
4	PEGMA	100	NaN_3	8000/80/80/80/2[e]	70	48	100	29000 (30000)	1.45
5	BA	100	NaN_3	8000/80/40/40/10	110	48	43	7400 (5600)	1.24
6	BA	100	BNSCN	8000/80/20/0/2	110	40	65	8600 (8300)	1.35
7	BA	100	NaOCN	8000/80/80/80/2	110	48	65	7300 (8300)	1.30

[a] Target degree of polymerization at 100% monomer conversion (calculated by [M]$_0$/[CP−I]$_0$). [b] M = monomer. [c]PMMA-calibrated GPC values. [d] Theoretical M_n calculated with [M]$_0$, [CP−I]$_0$, and monomer conversion. [e] Diluted with toluene (50% PEGMA and 50% toluene).

Table 3. One-Pot Synthesis of Chain-End Functionalized Polymers.

Entry	Target DP[a]	Catalyst	$[MMA]_0/[CP-I]_0/[catalyst]_0/[crown\ ether]_0/[I_2]_0$ (mM)	Solvent	T (°C)	t (h)	Conv (%)	M_n ($M_{n,theo}$[b])	PDI
1	30	NaN_3	8000/270/300/300/3	toluene[c]	70	3	79	3100 (2400)	1.17
				+ DMF[d]	rt	12	–	3400	1.16
2	50	NaN_3	8000/160/180/180/2	toluene[c]	70	5	84	5000 (4200)	1.17
				+ DMF[d]	rt	12	–	5300	1.15
3	100	NaN_3	8000/80/90/90/1	toluene[c]	70	10	83	8400 (7600)	1.16
				+ DMF[d]	rt	12	–	8200	1.19
4	30	BNSCN	8000/270/330/0/3	toluene[c]	70	8	74	2600 (2200)	1.19
				+ DMF[d]	60	12	–	2700	1.21

[a] Target degree of polymerization at 100% monomer conversion (calculated by $[MMA]_0/[CP-I]_0$). [b] Theoretical M_n calculated with $[MMA]_0$, $[CP-I]_0$, and monomer conversion. [c] Solution polymerization with toluene (25%) and MMA (75%). [d] Addition of DMF to the polymerization solution (DMF/polymerization solution = 2/1). The M_n and PDI values are those after purification by reprecipitation.

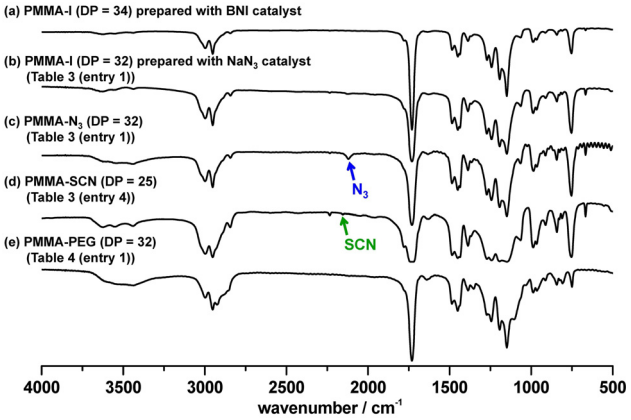

Figure 8. IR spectra of PMMA-I obtained with (a) BNI and (b) NaN_3 catalysts, (c) PMMA-N_3, (d) PMMA-SCN, and (e) PMMA-PEG. The reaction conditions are given in Tables 3 and 4.

The infrared (IR) spectrum of the polymer after the chain-end transformation showed a characteristic absorption band for N_3 at 2120 cm^{-1} (Figure 8c), demonstrating the successful generation of PMMA−N_3. The polymer obtained after the polymerization showed virtually no absorption of N_3 (Figure 8b), and the spectrum matched that of a PMMA−I independently synthesized using the BNI catalyst under an azide-free condition (Figure 8a). Thus, the chain-end transformation occurred only after the addition of DMF (a polar solvent). Substitution may occur by an S_N2 mechanism or be mediated by DMF via an S_N1 or SET mechanism.

The obtained polymers were further analyzed by ^1H NMR (Figure 9). The methyl protons at the side chain appeared at 3.52-3.80 ppm. After the polymerization (Figure 9a), a down-field peak at 3.73-3.76 ppm appeared and is assigned to the ω-terminal chain-end unit (a') adjacent to iodide. This assignment was previously confirmed with a PMMA−I synthesized in an azide-free condition.[43] After the chain-end transformation (Figure 9b), the peak was shifted furhter downfield to 3.74-3.80 ppm, which is most likely assigned to the chain-end unit (a") adjacent to N_3. Although this assignment is not definitive, the observed peak shift suggests the transformation of the chain end. The polymer after the polymerization (Figure 9a) displayed a minor peak at 3.74-3.80 ppm for N_3, but the peak was rather small, confirming high fidelity of iodide chain-end during the polymerization.

We attempted to use matrix-assisted laser desorption/ionization time-of-flight mass spectrometry (MALDI-TOF-MS) for further analysis. However, the carbon-iodide[44] and carbon-azide bonds were so weak that the bonds could be cleaved during the MALDI-TOF-MS analysis, and useful spectra were not obtained.

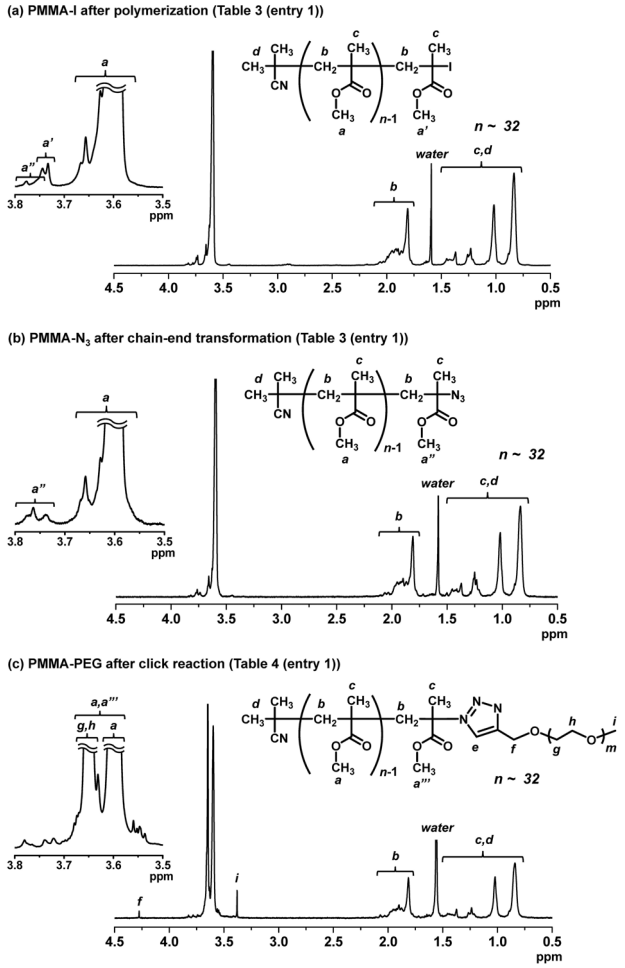

Figure 9. ^1H NMR spectrum ($CDCl_3$) of (a) PMMA-I obtained after the polymerization in toluene and (b) PMMA-N_3 obtained after the addition of DMF, and (c) PMMA-PEG obtained after click reaction. The reaction conditions for (a) and (b) are given in Table 3 (entry 1). The reaction condition for (c) is given in Table 4 (entry 1).

For quantitative characterization, the polymer after the transformation was studied by elemental analysis (EA) (Table 4 (entry 1)). N(exp) is the nitrogen content experimentally determined by EA. N(theo) is the nitrogen content theoretically calculated from the M_n determined by GPC and on the assumption that all of the polymer chains possess N_3 at the growing chain end and a cyano-containing CP group at the initiating chain end. The fraction of N_3 at the chain end (Table 4) was calculated by (N(exp) – N(theo)×1/4)/(N(theo)×3/4) to be 90% (with 10% experimental error), confirming a high yield of PMMA−N_3.

A chain-extension experiment was conducted with the polymers after the polymerization (PMMA−I) and the chain-end transformation (PMMA−N_3). These polymers were used as macroinitiators in the polymerization of MMA with a tetraoctylammonium iodide (ONI) catalyst at 60 °C. Figure 10 shows the GPC chromatograms at 0 and 3 h. A large fraction of the PMMA−I macroinitiator (Figure 10a) extended to a high molecular weight. Only a minor peak remained for the starting peak and is attributed to terminated chains and PMMA−N_3 generated during the polymerization. Upon the peak resolution, we estimated these inactive polymers (terminated chains and PMMA−N_3) to be at most 10%, again confirming the high fidelity of the iodide chain-end during the polymerization. In contrast, the chain did not extend with the polymer after the chain-end transformation (Figure 10b), indicating that all of the PMMA−I was converted to PMMA−N_3 after the chain-end transformation.

We prepared PMMA−N_3 with higher DPs (= 51 and 80), as shown in Tables 3 and 4 (entries 2 and 3) (Supporting Information (Figures S9 and S10)). The fraction of N_3 at the chain end was 93% and 99% (with 10% experimental error), respectively, showing high yields of PMMA−N_3. These results clearly demonstrate the successful one-pot synthesis of PMMA−N_3 in high yields (90-99%) by simply altering the solvent quality.

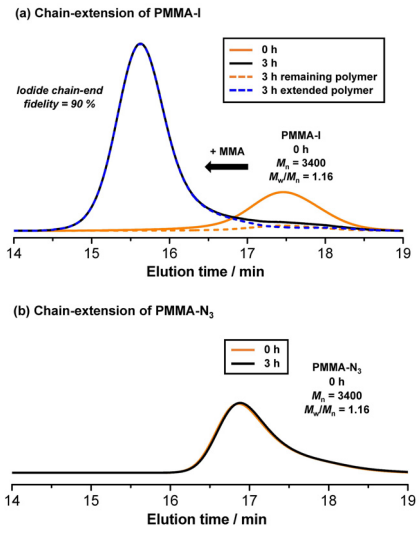

Figure 10. GPC chromatograms for the MMA/PMMA-X/ONI system (60 °C) for 0 and 3 h: $[MMA]_0$ = 8 M; $[PMMA\text{-}X]_0$ = 80 mM; $[ONI]_0$ = 80 mM. PMMA-X is (a) PMMA-I and (b) PMMA-N_3 prepared in Table 3 (entry 1).

The amount of NaN_3 used in the present experiments was 1.1 equivalent to PMMA−I. This amount is much smaller than the previously reported amount (10-fold excess of NaN_3) used to convert polymethacrylate-bromide to polymethacrylate-N_3. The dramatic reduction of NaN_3 in the present case would be attributed to the use of iodide (PMMA−I), offering a practically attractive route for synthesizing polymethacrylate-N_3.

Besides N_3, we also used BNSCN to carry out a one-pot synthesis of PMMA−SCN (Table 3 (entry 4)) (Supporting Information (Figure S10)). We obtained a PMMA−SCN with M_n = 2700 and PDI = 1.21. For the chain-end transformation, we used a higher temperature for SCN (60 °C) than N_3 (room temperature), because the nucleophilicity of $^-$SCN is weaker than that of N_3^-. SCN was observed in the IR spectrum at 2155 cm^{-1} (Figure 8d).

Alkyl thiocyanates (R–SCN) are used as important precursors for synthesizing various sulfur-containing compounds such as thiols, thioesters, disulfides, and sulfur-containing heterocycles.[45,46] R–SCN also undergoes an addition reaction to alkynes, enabling R to connect various molecules.[45] Thus, the obtained polymer–SCN is an attractive precursor for designing functional polymers.

The SCN anion is an ambident nucleophile taking $^-$SCN and $^-$NCS forms. Therefore, R–SCN and R–NCS are obtainable through the nucleophilic substitution. R–NCS is thermodynamically more stable and could be obtained at high temperatures.[45] However, because the nucleophilicity of the sulfur ($^-$SCN) is higher than that of the nitrogen ($^-$NCS), R–SCN is exclusively obtainable under mild reaction conditions, under which the isomerization of R–SCN to R–NCS is avoided.[45] Under the present mild condition, the formation of PMMA–NCS would be negligible.

Synthesis of Block Copolymers via Azide-Alkyne Click Reaction. Using an azide-alkyne cycloaddition click reaction, we synthesized an amphiphilic block copolymer. PMMA−N_3 (M_n = 3400 and PDI = 1.16) (Table 3 (entry 1)) (1 eq) was reacted with an alkyne-bearing polyethylene glycol (PEG) (M_n = 1000 and PDI = 1.06) (1.5 eq) in the presence of a copper (CuBr) catalyst (1.5 eq) in tetrahydrofuran (THF) at room temperature. To dissolve CuBr in THF, we added *N*,*N*,*N*',*N*'',*N*''-pentamethyldiethylenetriamine (2 eq). After 24 h, we successfully obtained a PMMA−PEG amphiphilic block copolymer with M_n = 4300 and PDI = 1.15 (after purification). The block copolymer was purified by reprecipitation in methanol/water (2/1) mixture; Figure 9c shows the NMR spectrum. The connected point (f) and the ethylene oxide units (g and h) of PEG clearly appeared at 4.28 ppm and 3.63-3.68 ppm, respectively. From the peak area for the methoxy units (a and a''') of PMMA and the ethylene oxide units (g and h) of PEG, the fraction of PMMA−PEG (over all PMMA chains) was calculated to be 97% (with an experimental error range of 87-100%) (Table 4 (entry 1)). The IR absorption of N_3 at 2120 cm^{-1} completely disappeared (Figure 8e), meaning quantitative consumption of N_3 through the click reaction. We also synthesized PMMA−PEG with longer PMMA chains (DP = 51 and 80) (Table 4 (entries 2 and 3) and Supporting Information (Figure S11)). The fraction of the PMMA−PEG chains was 94% and 82%, respectively. These results demonstrate successful synthesis of PMMA−PEG block copolymers in high yields.

Table 4. Chain-End Functionality of PMMA−N_3.

Entry	Polymer[a]	N(exp) (%)	N(theo) (%)	Fraction of N_3 chain end (%) estimated by EA	Fraction of N_3 chain end (%) estimated from PEG-functionalization[b]
1	PMMA−N_3 (DP = 32)	1.25	1.40	90%	97%
2	PMMA−N_3 (DP = 51)	0.94	0.99	93%	94%
3	PMMA−N_3 (DP = 80)	0.65	0.61	99%	82%

[a] Synthetic conditions are given in Table 3. [b] A mixture of PMMA−N_3 (10 wt%) (1 eq), 3-(poly(ethylene)glycol)-prop-1-yne (1.5 eq), CuBr (1.5 eq), *N*,*N*,*N*',*N*'',*N*''-pentamethyldiethylenetriamine (2 eq), and THF (90 wt%) was stirred at room temperature for 24 h.

Table 5. One-Pot Synthesis of N_3-Chain-End Functionalized Polymer Brushes on Surface.

Entry	Target surface coverage of N_3	$[MMA]_0/[CP-I]_0/[NaN_3]_0$ / $[crown\ ether]_0$ (mM)[a]	t (h)[a]	Conv (%)[b]	M_n[c] ($M_{n,theo}$[d])	PDI[c]	Thickness (nm)	Graft density (σ) (chain nm^{-2})	Surface occupancy (σ*)
1	100%	8000/40/40/40	16	81	17400 (16300)	1.32	7.0	0.29	0.16
2	75%	8000/40/30/30	20	87	18700 (17400)	1.35	8.0	0.31	0.17
3	50%	8000/40/20/20	24	74	15400 (14700)	1.35	8.8	0.41	0.23

[a] Polymerization condition. The solvent was toluene (MMA/toluene = 75/25). [b] Monomer conversion after the polymerization. [c] M_n and PDI values of free polymers after the chain-end transformation. The chain-end transformation was conducted by the addition of DMF (polymerization solution/DMF = 1/2); the reaction solution was stirred at room temperature for 24 h. [d] Theoretical M_n calculated with $[MMA]_0$, $[CP-I]_0$, and monomer conversion.

Assuming that the click reaction is quantitative, these results in turn indicate high yields of PMMA−N_3 after the above mentioned reaction of PMMA−I with NaN_3 in DMF. The fraction of N_3 at the chain end estimated by EA and PEG-functionalization was 82-99% in the three studied cases (Table 4), again confirming the successful one-pot synthesis of PMMA−N_3 in high yields.

One-Pot Synthesis of Azide-Chain-End Functionalized Polymer Brushes on Surface. The one-pot synthesis was applied to obtain N_3-chain-end functionalized polymer brushes on a surface. A unique aspect studied was the control of the N_3 coverage.

The surface of a material plays crucial roles in many important properties such as thermodynamic, mechanical, chemical, and biological properties as an interface to external phases.[47–51] Surface-initiated graft polymerization, in which polymerization is conducted from an initiator bound to a surface, is among the most effective surface modification methods. The use of LRP in surface-initiated graft polymerization can afford a polymer brush with a high surface density. Such a so-called concentrated polymer brush[47] takes a highly extended chain conformation so that the chain end tends to be localized at the outermost surface of the brush layer. Thus, the chain-end can effectively interact with external phases. Such localization is not attainable by conventional semi-dilute and dilute brushes.

We conducted a one-pot synthesis of N_3-functionalized polymer brushes on a surface. We used a surface-immobilizing initiator, 6-(2-iodo-2-isobutyloxy)hexyltriethoxysilane (IHE) (Figure 11a), consisting of an alkyl iodide (initiating) moiety and a triethoxysilyl (TEOS) group. IHE was fixed on a silicon wafer through the TEOS group. The IHE-immobilized silicon wafer was immersed in a mixture of MMA, a non-immobilized free initiator CP−I, NaN_3, crown ether, and toluene (solvent) and heated at 70 °C for the polymerization (Table 5). The free initiator CP−I was added because its addition can improve the control over the M_n and PDI of the graft polymer. The M_n and PDI of the free polymers generated from the free initiators are usually in good agreement with those of the graft polymers.[47] The molar ratio of NaN_3 to CP−I was varied from 1.0 (entry 1), 0.75 (entry 2), to 0.5 (entry 3). After 16-24 h, the monomer conversion reached 74-87%.

Subsequently, DMF was added to the polymerization solution for the chain-end transformation at room temperature for 24 h. The M_n and PDI values of the obtained free polymers were 15,400-18,700 and 1.32-1.35, respectively. The thickness of the brush was measured to be 7.0-8.8 nm using atomic force microscopy (AFM). We scratched the brush and measured the height gap between the scratched and unscratched areas (Figure 11b). Assuming the same M_n for the graft and free polymers, the surface density of the graft polymer was calculated to be 0.29-0.41 chains/nm^2 (the surface occupancy σ^* was 0.16-0.23) (Table 5). This density is high and located in a concentrated polymer brush region, indicating the successful synthesis of concentrated polymer brushes.

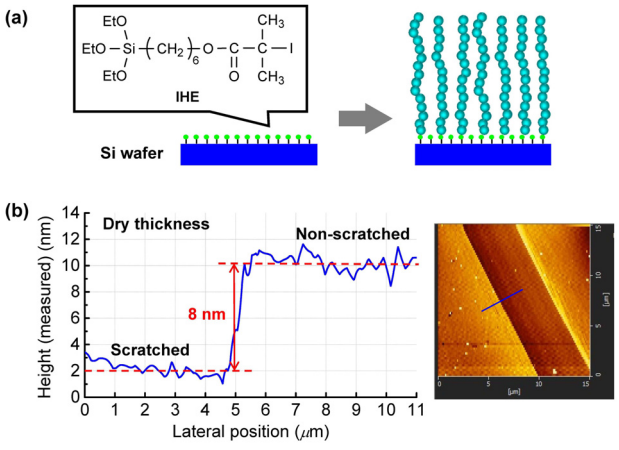

Figure 11. Surface-initiated graft polymerization of MMA. The experimental condition is given in Table 5 (entry 2). (a) Schematic illustration and (b) AFM height profile in the scratched and non-scratched areas of obtained brush.

We varied the molar ratio of NaN_3 to CP−I from 0.5, 0.75, to 1.0 for controlling the chain-end functionality of N_3 from 50%, 75%, to 100%. Because the number of brush polymers is much smaller than that of the free polymer, the N_3 functionality of the brush polymer is virtually the same as that of the free polymer and is thus controllable by the molar ratio of NaN_3 to the free initiator CP−I. Precise control of the N_3 functionality of the brush is difficult without the free polymer, because the number of the graft polymer is extremely small. The present method enables precise fractional control of the N_3-functionality of the brush by simply altering the molar ratio of NaN_3 to CP−I.

The N_3-functionalized brushes were reacted with alkynes bearing PEG and a fluorinated alkyl (C_8F_{17}) group for obtaining PEG- and C_8F_{17}-functionalized brushes. Figure 12 shows the contact angle (θ) of a water droplet on the brushes. The θ value was 79 degrees for all of the 50, 75, and 100% N_3-functionalized brushes (circles). After the PEG (hydrophilic) (squares) and C_8F_{17} (super-hydrophobic) (triangles) functionalization, the θ value clearly decreased and increased, respectively, with an increase of the surface functionality. This result clearly demonstrates the successful fractional control of the N_3, PEG, and C_8F_{17} functionalities of the polymer brush. This fractional control may also be applied to molecular bottle brushes and hyper-branched polymers, which will be studied in our group.

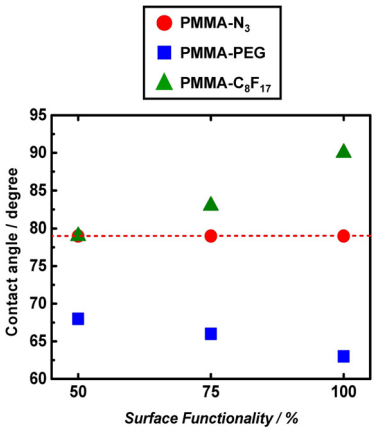

Figure 12. Plot of contact angle vs surface coverage of N_3, PEG, and C_8F_{17} on PMMA brushes. The symbols are indicated in the figure. The preparation of the samples is given in Table 5.

The C_8F_{17} functionalization of the brush was also confirmed by X-ray photoelectron spectroscopy (XPS) analysis (Supporting Information (Figure S12)), which clearly exhibited the F 1s signal.

CONCLUSIONS

R–I reacted with N_3^-, $^-$SCN, and $^-$OCN to reversibly generate $R^\bullet$ in non-polar solvents. With this new reaction, these anions were employed as efficient catalysts for LRP. The reaction of R–I with N_3^- and $^-$SCN was solvent-selective, generating substitution products (R−N_3 and R−SCN) in polar solvents. Exploiting this solvent selectivity, the one-pot synthesis of PMMA−N_3 and PMMA−SCN was achieved with the dual use of N_3^- and $^-$SCN as polymerization catalysts in a non-polar solvent and substitution agents in a polar solvent. The one-pot synthesis was also applied to surface-initiated polymerization, uniquely attaining the fractional control of the N_3 functionality of the polymer brush in the desired manner. Through the N_3 functionality, the linear and brush polymers can be connected to various molecules such as biological molecules and sensing probes, possibly offering advanced materials. The facile operation, access to unique polymer designs, and no requirement for excess NaN_3 are highly beneficial in various applications.

ASSOCIATED CONTENT

Supporting Information

Experimentals, syntheses of CP−N_3, EMA−N_3, and functional alkynes, polymerizations of MMA with lower concentrations of NaN_3, polymerizations of MMA for higher molecular weights, and spectral (IR, NMR, and XPS) data. This material is available free of charge via the Internet at http://pubs.acs.org.

AUTHOR INFORMATION

Corresponding Author

*agoto@ntu.edu.sg

Notes

The authors declare no competing financial interest.

ACKNOWLEDGMENTS

This work was partly supported by Start-Up-Grant of Nanyang Technological University.

REFERENCES

(1) Cram, D. J.; Rickborn, B.; Kingsbury, C. A.; Haberfield, P. *J. Am. Chem. Soc.* **1961**, *83*, 3678–3687.
(2) Poon, T.; Sivaguru, J.; Franz, R.; Jockusch, S.; Martinez, C.; Washington, I.; Adam, W.; Inoue, Y.; Turro, N. J. *J. Am. Chem. Soc.* **2004**, *126*, 10498–10499.
(3) Huang, Y.; Wayner, D. D. M. *J. Am. Chem. Soc.* **1994**, *116*, 2157–2158.
(4) Nguyen, N. H.; Levere, M. E.; Kulis, J.; Monteiro, M. J.; Percec, V. *Macromolecules* **2012**, *45*, 4606–4622.
(5) Bräse, S.; Gil, C.; Knepper, K.; Zimmermann, V. *Angew. Chem. Int. Ed.* **2005**, *44*, 5188−5240.
(6) Kolb, H. C.; Finn, M. G.; Sharpless, K. B. *Angew. Chem. Int. Ed.* **2001**, *40*, 2004−2021.
(7) Meldal, M.; Tornøe, C. W. *Chem. Rev.* **2008**, *108*, 2952–3015.
(8) Goto, A.; Ohtsuki, A.; Ohfuji, H.; Tanishima, M.; Kaji, H. *J. Am. Chem. Soc.* **2013**, *135*, 11131−11139.
(9) Sarkar, J.; Xiao, L.; Goto, A. *Macromolecules* **2016**, *49*, 5033−5042.
(10) Ohtsuki, A.; Lei, L.; Tanishima, M.; Goto, A.; Kaji, H. *J. Am. Chem. Soc.* **2015**, *137*, 5610−5617.
(11) Goto, A.; Zushi, H.; Hirai, N.; Wakada, T.; Tsujii, Y.; Fukuda, T. *J. Am. Chem. Soc.* **2007**, *129*, 13347−13354.
(12) Goto, A.; Suzuki, T.; Ohfuji, H.; Tanishima, M.; Fukuda, T.; Tsujii, Y.; Kaji, H. *Macromolecules* **2011**, *44*, 8709-8715.
(13) Tasdelen, M. A.; Kahveci, M. U.; Yagci, Y. *Prog. Polym. Sci.* **2011**, *36*, 455−567.

(14) Debuigne, A.; Hurtgen, M.; Detrembleur, C.; Jérôme, C.; Barner-Kowollik, C.; Junkers, T. *Prog. Polym. Sci.* **2012**, *37*, 1004−1030.
(15) Matyjaszewski, K.; Möller, M. *Polymer Science: A Comprehensive Reference*; Elsevier: Amsterdam, 2012.
(16) Tsarevsky, N. V.; Sumerlin, B. S. *Fundamentals of Controlled/Living Radical Polymerization*; Royal Society of Chemistry: U.K., 2013.
(17) Matyjaszewski, K.; Tsarevsky, N. V. *J. Am. Chem. Soc.* **2014**, *136*, 6513−6533.
(18) Ouchi, M.; Sawamoto, M. *Macromolecules* **2017**, *50*, 2603−2614.
(19) Boyer, C.; Corrigan, N. A.; Jung, K.; Nguyen, D.; Nguyen, T.-K.; Adnan, N. N. M.; Oliver, S.; Shanmugam, S.; Yeow, J. *Chem. Rev.* **2016**, *116*, 1803−1949.
(20) Zhang, N.; Samanta, S. R.; Rosen, B. M.; Percec, V. *Chem. Rev.* **2014**, *114*, 5848−5958.
(21) David, G.; Boyer, C.; Tonnar, J.; Ameduri, B.; Lacroix-Desmazes, P.; Boutevin, B. *Chem. Rev.* **2006**, *106*, 3936−3962.
(22) Nicolas, J.; Guillaneuf, Y.; Lefay, C.; Bertin, D.; Gigmes, D.; Charleux, B. *Prog. Polym. Sci.* **2013**, *38*, 63−235.
(23) Keddie, D. J.; Moad, G.; Rizzardo, E.; Thang, S. H. *Macromolecules* **2012**, *45*, 5321−5342.
(24) Yamago, S. *Chem. Rev.* **2009**, *109*, 5051−5068.
(25) Satoh, K.; Kamigaito, M. *Chem. Rev.* **2009**, *109*, 5120−5156.
(26) Monteiro, M. J.; Cunningham, M. F. *Macromolecules* **2012**, *45*, 4939−4957.
(27) Mastan, E.; Li, X.; Zhu, S. *Prog. Polym. Sci.* **2015**, *45*, 71−101.
(28) Zetterlund, P. B.; Thickett, S. C.; Perrier, S.; Bourgeat-Lami, E.; Lansalot, M. *Chem. Rev.* **2015**, *115*, 9745−9800.
(29) Chen, M.; Zhong, M.; Johnson, J. A. *Chem. Rev.* **2016**, *116*, 10167−10211.
(30) Goto, A.; Fukuda, T. *Prog. Polym. Sci.* **2004**, *29*, 329−385.
(31) Golas, P. L.; Matyjaszewski, K. *Chem. Soc. Rev.* **2010**, *39*, 1338–1354.
(32) Fournier, D.; Hoogenboom, R.; Schubert, U. S. *Chem. Soc. Rev.* **2007**, *36*, 1369−1380.
(33) Coessens, V.; Matyjaszewski, K. *J. Macromol. Sci., Part A. Pure Appl. Chem.* **1999**, *A36*, 667−679.
(34) Mukherjee, A.; Tothadi, S.; Desiraju, G. R. *Acc. Chem. Res.* **2014**, *47*, 2514−2524.
(35) Cavallo, G.; Metrangolo, P.; Milani, R.; Pilati, T.; Priimagi, A.; Resnati, G.; Terraneo, G. *Chem. Rev.* **2016**, *116*, 2478−2601.
(36) Savéant, J.-M. *J. Am. Chem. Soc.* **1987**, *109*, 6788−6795.
(37) Lund, T.; Lund, H. *Acta. Chem. Scand.* **1988**, *B42*, 269−279.
(38) Balslev, H.; Daasbjerg, K.; Lund, H. *Acta. Chem. Scand.* **1993**, *47*, 1221−1231.
(39) Percec, V.; Popov, A. V.; Ramirez-Castillo, E.; Coelho, J. F. J.; Hinojosa-Falcon, L. A. *J. Polym. Sci., Part A: Polym. Chem.* **2004**, *42*, 6267−6282.
(40) Moad, G.; Rizzardo, E. *Macromolecules* **1995**, *28*, 8722−8728.
(41) Goto, A.; Fukuda, T. *Macromol. Rapid Commun*. **1999**, *20*, 633−636.
(42) Tang, W.; Kwak, Y.; Braunecker, W.; Tsarevsky, N. V.; Coote, M. L.; Matyjaszewski, K. *J. Am. Chem. Soc.* **2008**, *130*, 10702−10713.
(43) Xiao, L.; Sakakibara, K.; Tsujii, Y.; Goto, A. *Macromolecules* **2017**, *50*, 1882−1891.
(44) Chen, C.; Xiao, L.; Goto, A. *Macromolecules* **2016**, *49*, 9425−9440.
(45) Castanheiro, T.; Suffert, J.; Donnard, M.; Gulea, M. *Chem. Soc. Rev. 2016*, **45**, 494−505.
(46) Erian, A. W.; Sherif, S. M. *Tetrahedron*, **1999**, *55*, 7957−8024.
(47) Tsujii, Y.; Ohno, K.; Yamamoto, S.; Goto, A.; Fukuda, T. *Adv. Polym. Sci.* **2006**, *197*, 1–45.
(48) Barbey, R.; Lavanant, L.; Paripovic, D.; Schuwer, N. Sugnaux, C.; Tugulu, S.; Klok, H. *Chem. Rev.* **2009**, *109*, 5437–5527.
(49) Goto, A.; Tsujii, Y. *Adv. Polym. Sci.* **2016**, *270*, 107–122.
(50) Zoppe, J. O.; Ataman, N. C.; Mocny, P.; Wang, J.; Moraes, J.; Klok, H. A. *Chem. Rev.* **2017**, *117*, 1105−1318.
(51) Chen, W-L; Cordero, R.; Tran, H.; Ober, C. K. *Macromolecules*, **2017**, *50*, 4089–4113.

TOC artwork

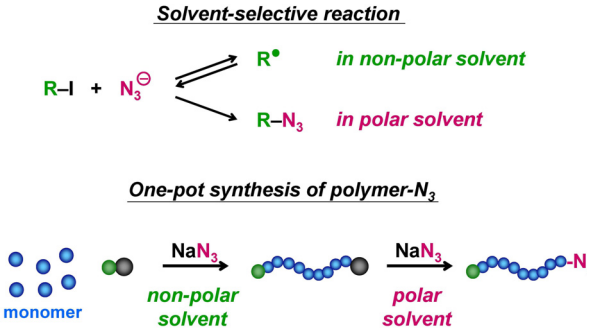
Solvent-selective reaction
R–I + $N_3^{\ominus}$
R•
in non-polar solvent
R–N_3
in polar solvent
One-pot synthesis of polymer-N_3
monomer
NaN_3
non-polar solvent
NaN_3
polar solvent
-N